Thermal properties of clay containing polymeric reinforcement as an eco-friendly bio-insulation composite for buildings

Souad Ghyati[1] · Said Kassou[2] · Mostapha El Jai[3,5] · El Hassan El Kinani[1] · Mabrouk Benhamou[4] · Sheng Hsiung Chang[2]

Abstract

Polymer/clay-based composites were prepared via solution intercalation method using natural clay and poly (ethylene) glycol (PEG4000) as organic dispersed phase. The present work consists of studying the effect of PEG content on the hybrids surface morphology, thermal stability and thermophysical properties. On the other hand, the TGA data and the measured thermophysical properties are, respectively, fitted with a logistic-like laws and virial expansions for different polymer contents. The results showed that the experimental data agree with the proposed theoretical models. Furthermore, the incorporation of the PEG chains into the clay matrix improves both the thermal stability and thermal characteristics of the raw clay. The thermophysical properties data showed that the elaborated hybrid acts as good thermal insulator for polymer contents higher than 2.5%. Finally, the resulting clay-based composite showed not only interesting characteristics in terms of insulation, but also satisfies both economic and environmental requirements.

Introduction

Building energy efficiency is increasingly becoming one of the main concerns, which attracts researchers and industrials from all over the world. A challenging goal in this field is to reduce the energy consumptions being more than 40% of the total energy demand [1]. Within this context, the building materials play an important role of a thermal filter allowing a conservation of indoor climate, independently of the outside fluctuations, especially, in the Mediterranean climatic conditions [2]. To achieve this goal, specific thermal insulation materials were encapsulated within the building envelope and constitute an alternative solution that should be taken into account [3–5] . In fact, thermal insulator is a material or combination of materials that envelope buildings and then contribute to retard the rate of the heat flow through conduction, convection or radiation [6]. Being exposed to different climate changes, these materials must guarantee not only acceptable thermal performance, but also high resistance to fire, low water vapor permeability, sound insulation as well as good impact on both environment and human health. Bulk organic or inorganic materials, such as polystyrene, silica, fiberglass and wood, are commonly used as thermal insulator exhibiting low thermal conductivity and densities [7–9]. Despite this, they are relatively heavy, easy to burn and made of toxic molecules [10–12]. In the last few years and quite naturally, several previous works concerning some adequate materials combinations improve and diversify the field of the thermal insulation. As a consequence, these new systems provide interesting thermophysical properties as well as improved mechanical characteristics, compared with bulk insulation materials [13–15]. Clay is the most abundant natural mineral resource in the world, which with its desirable properties, such as durability, strength,

✉ Said Kassou
  saidkassou1@gmail.com

[1] ENSAM, Moulay Ismail University, P.O.Box 15290, Meknes, Al Mansour, Morocco

[2] Department of Physics, RD Center for Membrane Technology and Center for Nanotechnology, Chung Yuan Christian University, Taoyuan 32023, Taiwan, ROC

[3] Euromed Institute of Technology, Euromed University of Fez, Fez, Morocco

[4] LPRILM, Physics Department, Faculty of Sciences, Moulay Ismail University, P.O.Box 11201, Meknes, Morocco

[5] Ecole Nationale Supérieure d'Arts & Métiers, Moulay Ismail University, Meknes, Morocco

thermal stability, sound insulation and fire resistance, gains considerable demand in different industrial fields when it is combined with other organic materials [16–19].

In recent years, there has been considerable interest in the use of clays and clay minerals as an integral part of construction materials to enhance not only the mechanical properties, but also to contribute towards evaluating the thermal insulation performances. For example, Mucahit Suctu et al. [20] have studied the thermal behavior of hollow clay bricks made up of paper waste. The latter shows improved thermal properties, illustrated by reduced value of thermal conductivity from 0.68 to 0.39 W m^{-1}K^{-1}, as the quantity of additives increases in such microporous brick material. within the same context, Feng Hu and his co-workers [21] gave an overview of recent progress in developing different hallow-structured materials such as polymer foams, blends of polymers and hollow silica particles, assembly of hollow silica particles and aerogels used for thermal insulation applications. They come to the conclusion that decreasing the voids size below 350 nm and increasing their density induces a confinement effect, which is responsible for the reduction of the thermal conductivities of all the studied types of hollow-structured materials. Furthermore, Pragya Gupta et al. [22] discussed both the thermal insulation and flame retardancy properties of the sepiolite clay and cellulose nanofibers-based aerogel. Through this investigation, the elaborated specimens have shown similar aerogel properties, such as low density (ranging from 11.5 to 32.5 Kg m^{-3}) and high-porosity level (99.2 − 98.3%), with good dimensional stability. Also, the authors concluded that this composites provides good thermal insulation properties in comparison with some conventional thermal insulation materials. Another promising approach in this same field is the combination of rigid polyurethane (PU) and different concentrations of montmorillonite nanoclay, aiming to achieve a synergistic effects in terms of the thermal insulation performance of the material [23]. Such a cellular nanocomposites demonstrate reduced values of thermal conductivity by the inclusion of nanoclays, with a higher reduction for 1 mass%. On the other hand, many authors such as Sundstrom, Bruggeman, Maxwell, Agari, etc., have tended, in the past decade, to focus on the development of theoretical and/ or empirical models in order to describe thermal conductivity phenomena of special reinforced composites [24–26]. Obviously, these models play an important role in estimating, for instance, the effect of particle volume fraction, size, shape and interfacial area on the thermal properties of hybrid materials [27]. However, a challenging and more accurate model, taking into account the relationship among thermal conduction networks, polymer chain motion and λ values, still be of great interest.

From the literature review reported below, one can see that the problem of energy efficiency in building is largely investigated. However, all of the insulation materials, used in the construction industry, are generally polymer-based materials, such as polystyrene, polymer-based aerogels and polyurethane foam. In addition, the building construction sector still faces different difficulties and challenges, such as the cost, thermal and mechanical properties, health problems, etc. In this same context, and in order to participate to enrich the debate, the present work brings a new idea consisted in developing sustainable composites, with natural clay-matrix reinforced by an appropriate polymer. Generally, the thermal performance and mechanical properties of raw clays are strongly dependent on their mineralogical composition [28]. But, the local natural clay used in the present work provides stable and homogeneous chemical structure [29]. Therefore, it is interesting to develop a structure from coupling clayey material and polymer chemistry. In fact, an appropriate polymer to be incorporated may be poly(ethylene glycol) (PEG), being a hydrophilic polymer that can be intercalated and adsorbed on clay surfaces, and thus a change in the chemical environment of clay galleries is provided. This modified structure yield to improved thermal characteristics. As a consequence, it can be considered as a key solution permitting to obtain good insulators having less environmental impacts and are relatively cheap. The present paper deals with an elaboration of new hybrid materials with a clayey matrix, in order to improve their thermal properties, for promised applications. PEG/natural clay hybrids were prepared using *direct solution intercalation method*. The prepared hybrids of PEG-intercalated clay, with different polymer contents, were characterized using *scanning electron microscope* (SEM) technique. On the other hand, the thermal properties of such composite models have been investigated by *differential scanning calorimetry* (DSC) and *thermogravimetric analysis* (TG) techniques. Moreover, a discussion of the future challenges of the new hybrid, as thermal insulation material in building envelope, was given by analyzing its thermal insulation properties, through a measurement of the main interesting quantities, as absolute density, thermal conductivity, heat capacity and thermal diffusivity. This paper is organized as follows. In Sect. 2, we present the materials under consideration, experimental techniques and modeling methodology conducted to analyze the polymer/clay–based hybrids. Section 3 is devoted to a discussion of the obtained results including the future challenges of the new hybrid material, as thermal insulator for buildings. Finally, some concluding remarks are drawn in the last section.

Materials and methods

Materials

The natural clay used in the present investigation was collected from Meknes region (north-central of Morocco). The

raw clayey material, as disordered powder, exhibits a total amount of organic matter of about 15.17%, determined after calcination at 950°C, for 1 *hour*, and the remaining clay sample was then characterized by *X-ray fluorescence* [29]. The latter reports the chemical composition, including SiO_2 (46.77mass%), CaO (14.56mass%), Al_2O_3 (11.49mass%), Fe_2O_3 (5.46mass%), MgO (2.46mass%), K_2O (1.8 mass%), and some other metal oxides. On the other hand, the polyglycole, selected to be a supporting matrix, was commercially purchased from SIGMA-ALDRICH Company (Germany). Its average molecular mass ranges from 3500 to 4500 mol/g, and the associated melting point ranges from 58 to 60°C.

Preparation of clay-based hybrids

In order to intercalate clay with polymer chains into the clay matrix, *six* different clay-PEG composites were prepared. According to literature [30–32], the intercalation of PEG chains into the clay galleries was achieved through an *adsorption mechanism*. To this end, a desired amount of PEG (8mass%) was added to distilled water in glass bottles and sealed. The bottles were shaken vigorously to complete the dissolution of PEG in water, during which the solution was placed on a rotating mixer for gentle mixing. The aqueous PEG solutions, of lower mass fraction (0.6, 1.2, 1.8, 2.5, 2.8 and 3.1mass%), were prepared by diluting the stock solution, with an additional amount of distilled water, after which, the diluted samples were mixed, for 1 *hour*, at 58 °*C*. On the other hand, a fixed amount of clay was added to distilled water and stirred, for 6 *hours*. The mixtures, of desired mass fractions, were prepared in glass vials, by adding diluted PEG solutions to the clay dispersions. The resulting ternary solutions were stirred, for 12 *hours*, at ambient temperature, and heated, for 6 *hours*, at 60°C. Finally, the obtained samples were centrifuged at 4000 rpm for 40 min. The remaining solid was washed and dried at 100°C for 12 *hours* and then fractionated into small pieces using agate mortar so as to conduct further analysis (Fig. 1).

Scaning electron microscopy (SEM)

The surface morphology of clay-PEG composite samples was studied using a scanning electron microscope (Thermo Scientific™ Quattro SEM instrument, Rabat, Morocco). In order to prepare samples for SEM analysis, approximately 0.01 g of a dried powdered sample was placed on standard mounts, which were 15 mm in diameter and 2 mm in depth, and then coated with a 1 − 2-nm-thick conductive layer of gold to prevent charging.
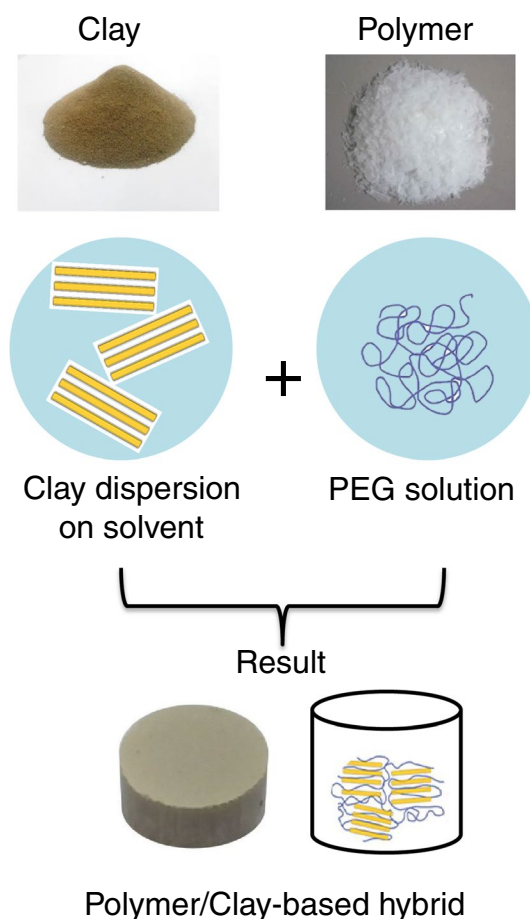

Fig. 1 Schematic diagram showing synthesis of polymer-clay hybrids

Thermal analysis

Thermogravimetric analysis (TGA), *differential thermal analysis* (DTA) and *derivative thermogravimetric analysis* (DTG) of the natural clay and composites were carried out using TG/DTA instrument (Shimatzu TA-60 thermal analyzer, Meknes, Morocco). The samples have an average mass of 27 mg, which were heated in aluminium pans in the range from room temperature to 600°C, with a ramp of 20°C and under an oxidative atmosphere.

The thermal characteristics of the new hybrids, such as melting and freezing points, latent heats and heat capacities, were evaluated using a *differential scanning calorimeter* (DSC) (TA Instrument Q1000 Tzero™ model, Fez, Morocco). A constant heating and cooling rate of 10°C min⁻¹ were adopted, the calibration constant was 1.0052, and the temperature accuracy was ±0.01°C. The measurements were conducted under a constant stream of nitrogen, at atmospheric pressure. Based on this technique, the heat capacity of the different hybrids is measured [33]. Once a scan has started, when $\Delta C \neq 0$, $\Delta T \neq 0$ and there is no phase transition, then the heat capacity is given as follows:

$$C = (dQ/dt)(\Delta t/\Delta T). \tag{1}$$

where dQ/dt and ΔT are the power applied to one face of each cell and the difference in temperature between the sample and the reference, respectively. The quantity $(\Delta t/\Delta T)$ is slope^{-1} of the output scan. If the power $dQ/dt = K_0$ is constant, then the heat capacity is given by:

$$C(\mathrm{JK}^{-1}) = K_0(slope)^{-1}. \tag{1a}$$

As a consequence, the heat capacity difference between the sample and reference is inversely proportional to the slope of the output scan.

Physical properties can have a strong influence on the thermal conduction behavior inside the hybrids. Therefore, absolute density of the different samples was measured using a gaz pycnometer (Micromeritics AccuPyc II 1340 , Meknes, Morocco) [34]. Cylindrical samples of 25 mm diameter and 20 mm thickness were analyzed 10 times at ambient temperature and under Helium gas (He). The samples were dried in the oven during 2 *hours* at 50°C before the density test.

The thermal conductivity was established through the *Guarded heat flow meter* (DTC-300 Stack) according to the procedure described in ASTM E1530 Standard [35]. The measurements were performed at room temperature and under atmospheric pressure. The results were reported as the average of three measurement values of the sample thermal conductivity.

The thermal diffusivity, D, is a physical quantity, characterizing the ability of a continuous material to transmit a temperature signal from one point to another inside it. Since the density, ρ, (in g cm^{-3} *unit*) of the sample, its thermal conductivity, λ, (in W m^{-1}K^{-1} *unit*) and specific heat capacity, C_P, (in J kg^{-1}K^{-1} *unit*) are known, the thermal diffusivity can be deduced by the following equation:

$$D(\mathrm{m}^2/\mathrm{s}) = \frac{1}{\rho}\frac{\lambda}{C_P}, \tag{2}$$

Thermal degradation modeling

TGA method has been widely used to determine the composition of multi-component systems, the decomposition temperature, the thermal stability, etc. To this end, it is interesting to give a simple theoretical model, which enable us to study the thermal stability and the thermal degradation behavior of the hybrid models versus polymer contents for each individual decomposition stage. In this context, we recall that the *residual mass*, $M(T)$, in percentage unit is given by

$$y(T) = 100 \times \frac{M(T)}{M_\mathrm{i}} , \tag{3}$$

where M_i denotes the initial mass of the sample. The mass loss, at temperature T, reads

$$\Delta M(T) = M_\mathrm{i} - M(T) . \tag{4}$$

In *percentage unit*, the mass loss is

$$z(T) = 100 \times \frac{M_\mathrm{i} - M(T)}{M_\mathrm{i}} . \tag{4a}$$

The goal, now, is to find a *closer* form for the residual mass, $M(T)$, in this temperature interval, and to compare it to that from experiment. For this purpose, we first assume that, in $T_\mathrm{i} - T_2$ temperature range, the residual mass solves the following *phenomenological* first-order differential equation

$$\frac{dM}{dT} = F(M) , \tag{5}$$

with the initial condition

$$M(T_\mathrm{i}) = M_\mathrm{i} , \tag{5a}$$

where M_i stands for the initial mass of the considered sample, before the thermal degradation of the latter takes place. Differential equation (5) means that the slope of the residual mass, at any temperature, is a function of this same residual mass. The M-dependent function, $F(M)$, is assumed to have good mathematical properties (continuity and derivability). In addition, we suppose that this function is analytic of the M variable. To second order in M, we adopt the polynomial form for function $F(M)$,

$$F_\mathrm{w}(M) = -k_\mathrm{w}M\left(1 - \frac{M}{M_\mathrm{w}}\right) . \tag{6}$$

Here, $k_\mathrm{w} > 0$ denotes the thermal degradation *rate* relatively to each decomposition stage. It is homogeneous to the inverse of temperature. Here, M_w is some positive adjustable parameter, with the condition that $M(T) < M_\mathrm{w}$, in temperature range $T_\mathrm{i} - T_1$ of interest, in order to ensure the monotone decreasing of the residual mass, $M(T)$, upon temperature. Then, differential equation (5) with the form (6) of function $F(M)$, is a *logistic equation* of *Verhulst* type [36], with the difference that the constant M_w does not play the role of the *medium capacity* (or capita). Hence, M_w may be viewed as a phenomenological constant. The Verhulst's differential equation can be solved exactly, and we simply give its solution, that is

$$M(T) = \frac{M_\mathrm{w}}{1 + e^{k_\mathrm{w}(T - T^*)}}, \qquad T_\mathrm{i} < T < T_1. \tag{7}$$

Here, $T^* < T_1$ is the *unique* inflection point of function $M(T)$. The phenomenological constant, M_w, can be experimentally measured through the formula

$$M_w = 2M^*, \tag{7a}$$

with the value of the residual mass at the inflection point, $M^* = M(T^*)$.

In $T_1 - T_2$ temperature range, where occurs the second decomposition stage, we write a similar *logistic* equation, but with other parameters, which are (M_p, k_p, T^{**}). We simply give the analytic expression of the residual mass, in this temperature-interval,

$$M(T) = \frac{M_p}{1 + e^{k_p(T-T^{**})}}, \qquad T_1 < T < T_2. \tag{8}$$

Here, $T^{**} < T_2$ accounts for a second *unique* inflection point. The phenomenological constant, M_p, can be experimentally measured via the formula

$$M_p = 2M^{**}, \tag{8a}$$

with $M^{**} = M(T^{**})$. There, the positive constant k_p denotes the thermal degradation *rate* relatively to the chemical decomposition of liquid polymer.

Let us comment about the above obtained solutions.

Firstly, the curves representing the residual mass, upon temperature, are *sigmoid*.

Secondly, they depend on *six* kinds of parameters, which are (M_w, k_w, T^*) and (M_p, k_p, T^{**}).

Thirdly, these parameters are not independent each other and must satisfy the following *two* equalities

$$\frac{M_w}{1 + e^{k_w(T_1-T^*)}} = \frac{M_p}{1 + e^{k_p(T_1-T^{**})}}, \tag{8b}$$

$$k_w\left(1 - \frac{M_1}{M_w}\right) = k_p\left(1 - \frac{M_1}{M_p}\right). \tag{8c}$$

These take into account the conditions of continuity of the residual mass and its first derivative at intermediate temperature, T_1, at which the first decomposition stage ends and the second one starts. Therefore, it will be sufficient to know only *four* parameters to determine all of the others.

Finally, we note that, at typical temperatures T^* and T^{**}, there is a drastic change of the thermal degradation velocity. It should be mentioned that, all these parameters depend naturally on the sample composition and can be determined by a fit with experimental data.

Results and discussions

Morphology

We first used SEM technique to investigate the surface morphology of the isolated clay particles, with and without added PEG. Such a qualitative tool provides photomicrographs indicating indirectly the interaction between polymer chains and clay layer surfaces or clay edges. The photographs of raw clay and clay-PEG hybrid samples are presented in Fig. 2.

The micrograph depicted in Fig. 2a describes the raw clay free from polymer chains, which is presented as adjacent fine particles of rather poorly crystallized kaolinite, some of them are made of well-oriented kaolinite layers. As it can be seen, in such *polydisperse* particles, even large kaolinite plates appear to be composed of much smaller platelets. This is in line with the result that is already reported by some authors [37]. They come out to the conclusion that more than 85% of kaolinite particles have particle size less than 0.5 μm.

Figure 2b–g indicates SEM photographs dealing with hybrid samples, of different PEG amounts. Images *b*, *c* and *d* corresponding to polymer fractions 0.6%, 1.2% and 1.8%, reveal that the clay particle size increases with increasing initial polymer concentration, in perfect agreement with our recent XRD observations and theoretical predictions [29]. At the polymer concentration 2.5% (image *e*), the micrograph of clay-PEG(w_4) hybrid shows that the space between the microparticles disappears and becomes completely connected through PEG chains. This phenomenon was attributed to the appearance of depletion forces between clay layers, which tend to repel the polymer chains from the interlayer galleries. As a consequence, the whole matrix becomes structurally durable and consolidated. Beyond, one can see that the particle size increases with the appearance of a well-ordered microstructure (image *f*) and the presence of typical spherical aggregates (image *g*) artificially formed during the elaboration process.

Thermogravimetric analysis

Figure 3 shows the coupled DTA and TG curves of the raw clay sample in terms of normalized mass loss, $(M_i - M)/M_i$. Under a change of temperature ranging from 25°C to 800°C, the sample demonstrates, progressively, different thermal losses according to *four* temperature regimes. In the *first regime*, where the temperature varies between 26°C and 120°C, we assist to a rapid decrease in the residual mass, with a mass loss of about 3.019%, which was attributed to a desorption of physically adsorbed water, located on the outer surface. In this same

Fig. 2 SEM photographs of
hybrids, with different polymer
mass fractions: **a** 0%, **b** 0.6%,
c 1.2%, **d** 1.8%, **e** 2.5%, **f** 2.8%,
and **g** 3.1%
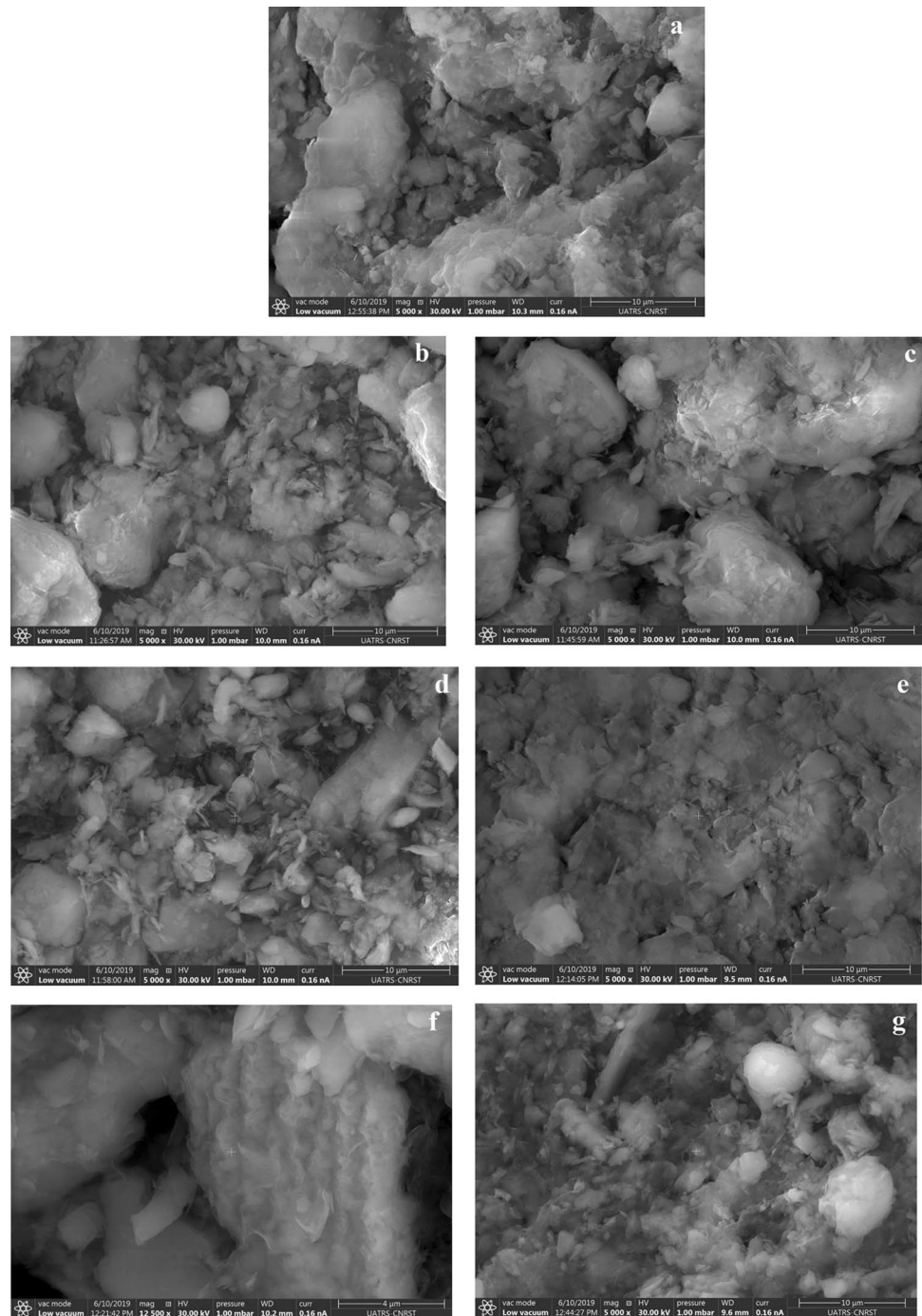
temperature range, DTA curve exhibits an endothermic peak with a minimum at 90°C. In the *second regime*, it was found that, in the temperature interval from 120°C to 200°C, a DTA endothermic peak was observed and is mainly linked to the desorption of the interlayer water. In the *third regime*, the clay mineral experienced a small mass loss of 0.591%, from 200 to 350°C. In such a regime,

exists a DTA endothermic peak, which is a signature of iron hydroxides dehydration. In the *fourth regime*, that is between temperatures 350°C and 700°C, where the mass loss is about 6.578%, a DTA endothermic peak is observed and indicates a dehydroxylation of structural water.

Finally, in the *last regime*, where temperature ranges from 700°C to 800°C, a mass loss is of about 5.283% was detected.

Fig. 3 DTA/TG plots associated with raw clay, upon temperature
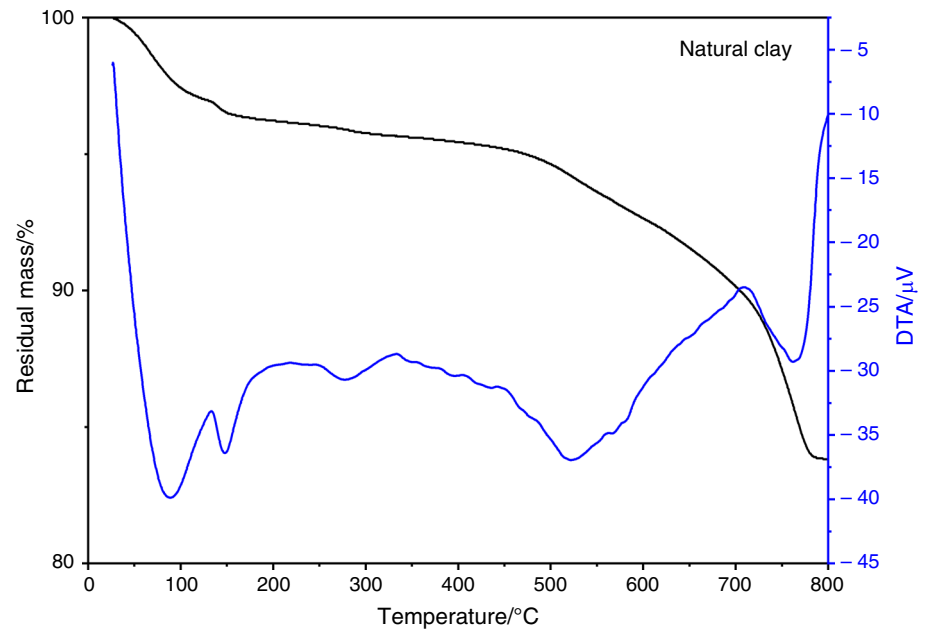
This loss can be attributed to the decomposition of the calcium carbonate mineral ($CaCO_3$).

Now, consider a clay-PEG hybrid, with different polymer mass fractions. Our question was how the thermal degradation of the new composite can be affected by a progressive addition of PEG.

Plots in Fig. 4 demonstrate that the clay-polymer hybrids degradation behaviors depend on the initial bulk polymer concentration, and it can be divided into *two* main stages. In the *first stage* (low-temperature regime), that is for temperatures ranging from $T_i = 26°C$ to some temperature, T_1, about 200°C, DTA curves show endothermic peaks corresponding, obviously, to the desorption of physically adsorbed water (component *w* (water)). Hereafter, we remark that the water mass loss of the hybrids

decreases with the polymer concentration and showed lower percentages compared with the raw clay. This is due to the fact that the water desorption process in such systems is essentially controlled by a confinement effect, in contrary to the raw clay, where the water desorption is rather a cooperative phenomenon. In the *second stage* (high-temperature regime), where temperature varies between $T_1 = 200°C$ and some temperature, T_2, about 400°C, there is a significant mass loss referred to the polymer decomposition (component *p* (polymer)). In this temperature range, the different DTA curves exhibit a series of exothermal peaks and give a strong evidence that the polymer in each sample follows different decomposition steps. Obviously, the associated losses become more relevant for higher polymer concentrations.

Table 1 summarizes the values the different TGA curves parameters of all the studied samples. This is done by fitting the above theoretical model to the experimental data.

On the other hand, in order to study the *thermal stability* of the different clay-PEG systems, Fig.5 deals with a comparison of measured (markers) and predicted (small dots) TGA data of natural clay and the various elaborated hybrids at temperatures ranging from $26°C$ to $400°C$. As can be seen from these curves, at temperatures below $50°C$, the degradation of PEG-intercalated clay hybrids highlighted by z_w values becomes less relevant compared to the raw clay. As a consequence, the high amount of polymer content provides negligible mass change, resulting in a good thermal stability. Furthermore, the decomposition of the PEG inside the clay matrix differs from the one of the pure PEG [38] and showed a clear decrease of the slop with lower onset thermal degradation T_1. For example, the degradation of the pure polymer started from $363.4°C$ and ended at $413.1°C$, while the samples of lower and higher polymer mass fractions: 0.6% and 3.1% demonstrates a degradation process at temperature ranges of $220.3 − 433.3°C$ and $181.0 − 421.8°C$, respectively. As a result, the thermal stability again was enhanced through the adsorption of high amount of polymer chains into the interlayer clay galleries.

Thermal characteristics

In this work, we have chosen DSC, because it is one of the most practical method used to study the thermal behavior and determining the thermal properties of hybrids. To this end, the present investigation focuses on such a developed technique for extracting the temperatures of the phase transition, such as melting-point, solidification onset, and latent heat of melting and freezing.
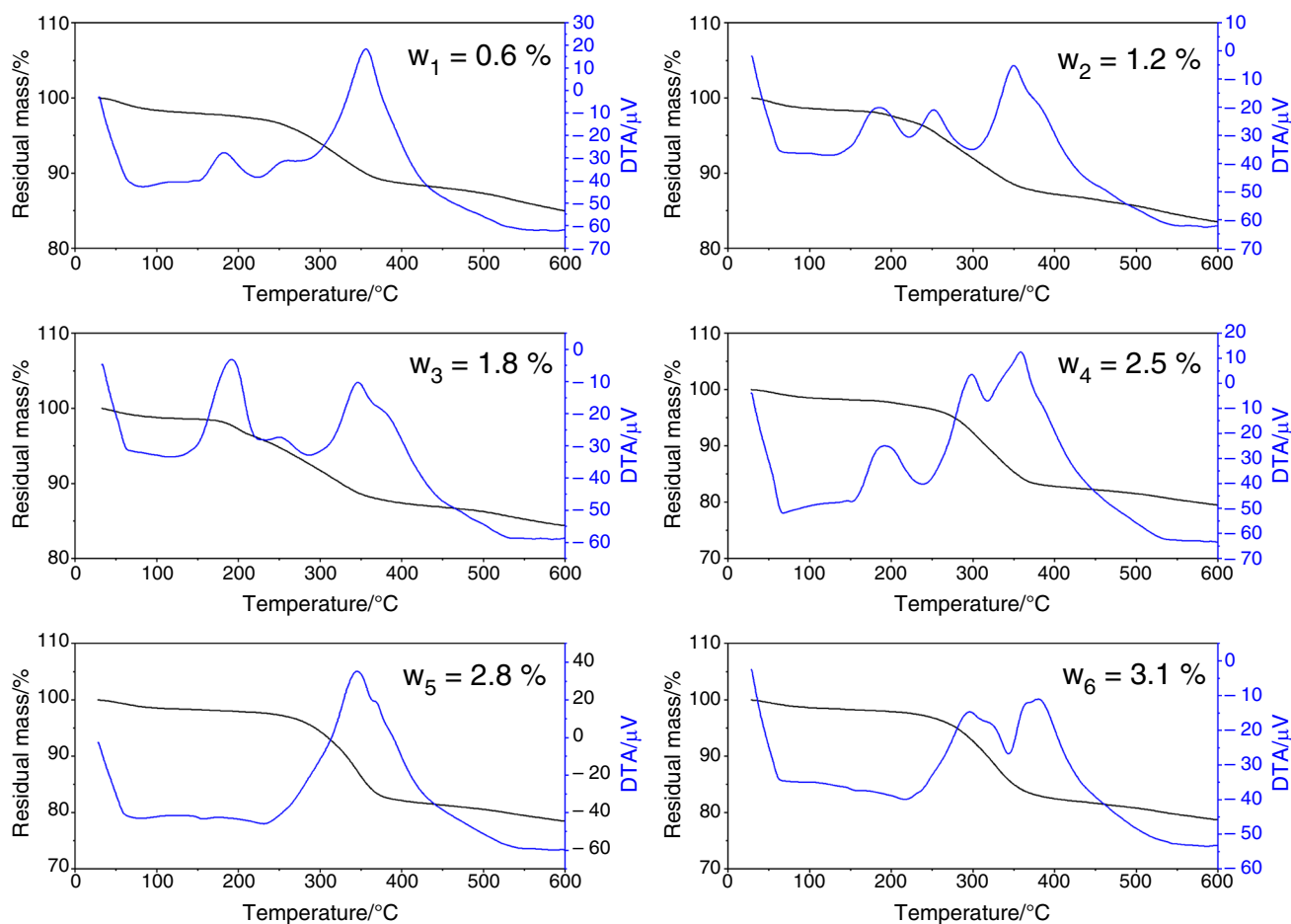
Fig. 4 DTA/TG curves of hybrids, upon temperature

Table 1 Values of parameters (M_w, k_w, T^*) and (M_p, k_p, T^{**}), relatively to the thermal degradation of raw clay and hybrids, obtained by a fit with experimental data

Samples	M_w /%	T^* /$^\circ$C	k_w /$^\circ$C^{-1}	M_P /%	T^{**} /$^\circ$C	k_p /$^\circ$C^{-1}	z_w /%	z_p /%
Raw clay	100.0	94.32	2.597	96.98	–	–	3.020	–
Clay-PEG$_{(w_1)}$	100.1	66.83	3.717	97.88	321.2	8.474	2.218	10.74
Clay-PEG$_{(w_2)}$	100.1	61.19	3.389	98.48	298.4	7.299	1.618	11.53
Clay-PEG$_{(w_3)}$	100.3	57.64	2.793	98.98	298.5	5.128	1.316	11.62
Clay-PEG$_{(w_4)}$	100.1	69.53	3.012	98.23	319.4	11.363	1.868	16.03
Clay-PEG$_{(w_5)}$	100.2	66.88	2.849	98.38	336.3	13.157	1.816	16.75
Clay-PEG$_{(w_6)}$	100.2	65.00	2.702	98.56	319.2	12.048	1.637	16.81

DSC curves of the raw clay and clay-PEG hybrids, provided during heating and cooling processes, between 20°C and 120°C, are, respectively, displayed in Figs. 6 and 7.

From Fig. 6, we observe that the thermal response of the raw clay is characterized by one endothermic event, observed at 38°C. As it is well known, such a peak is attributed to physically adsorbed water.

Plots in Fig. 7 reveal, first, that an increase of the polymer concentration in hybrid systems leads to enhanced latent heat of melting. It should be noted that the external

PEG is in solid state, while the intercalated one is in pasty state. Since PEG chains are highly cohesive, due to the monomers abundance, therefore, the latter requires a higher latent heat of fusion, as the concentration of the polymer increases.

Second, this same figure tell us that, as the polymer concentration is increased, the temperature of the fusion onset of the intercalated polymer diminishes, due to its plasty state, caused by the encapsulated water content.
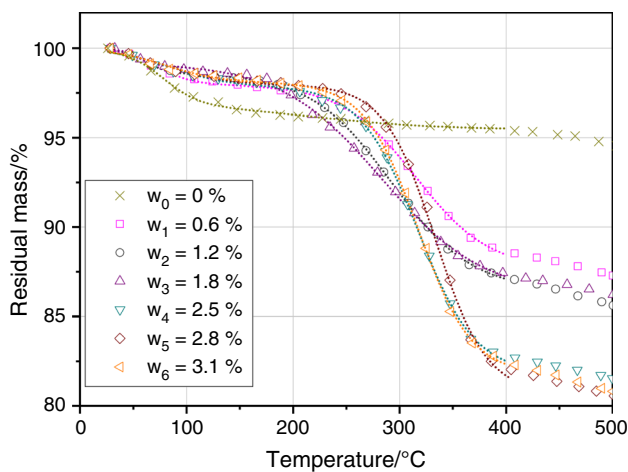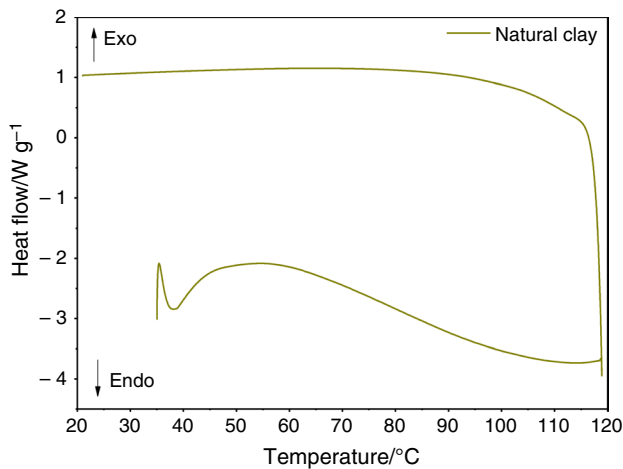
Fig. 5 Comparison of measured (markers) and predicted (small dots) TGA data of natural clay and the different hybrids
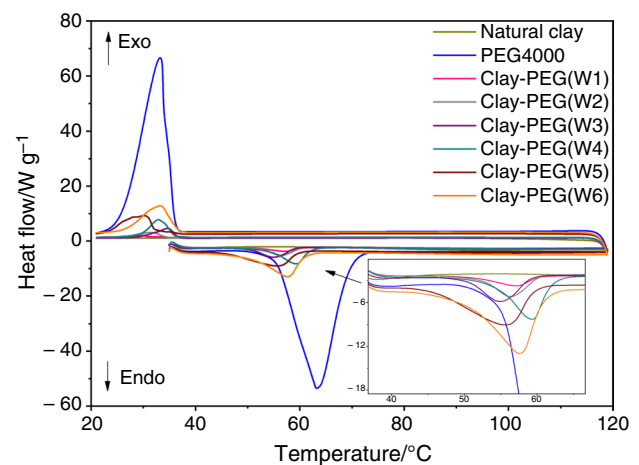
Fig. 7 Comparison between DSC curves, related to natural clay, pure PEG and hybrids, in temperature range 20–120 °C

Fig. 6 DSC curve of natural clay in temperature range 20–120 °C

Third, we have made a comparison of freezing temperatures relatively to pure and intercalated PEG (for different initial bulk-polymer-concentrations). DSC measurements suggest that the freezing temperature of the intercalated polymer increases with increasing polymer concentration and is greater than that of pure PEG. Then, the crystallization occurs at high temperature, since the intercalated polymer is in restricted geometry. We expect that the freezing temperature, T_F, of the intercalated PEG behaves as

$$T_F = T_F^0 + A w_i^x, \tag{9}$$

with an exponent $x > 0$ and the numerical factor $A > 0$. Here, $T_F^0 = 34.5°C$ refers to the freezing temperature of pure PEG, and w_i denotes the initial polymer concentration.

Fourth, as indicated in this figure, the incorporating PEG into the clayey matrix contributes to reduce the temperature range between melting and freezing onsets, opening up the possibility to use this new fabricated material, as a high temperature thermal energy storage material, especially in building envelope, under different climatic conditions.

Finally, Table 2 highlights the thermal characteristics of PEG-intercalated clay samples from DSC analysis. This table, together with Fig. 8, indicates that the latent heat of melting and freezing were found to be 181.3 and $-159.7 \, gJ^{-1}$, for PEG. Regarding the clay-PEG hybrids, the associated values tend to increase with the polymer concentration, leading to an enhanced energy storage percentage of about 79.4%.

Thermophysical properties

Density measurements

The building industry is interested in measuring the absolute density of lightweight composite insulating materials due to its process importance for each study. The absolute density, ρ_A, or more accurately the true density of samples is measured using helium pycnometry. In the present study, the identification of such a physical property is of great importance. To determine the absolute density, it is necessary to measure the mass of the sample [39]. The mass of the studied samples, m_S, was weighed in the dry state using an electrical balance. Then, the absolute density is calculated based on Boyle's law:
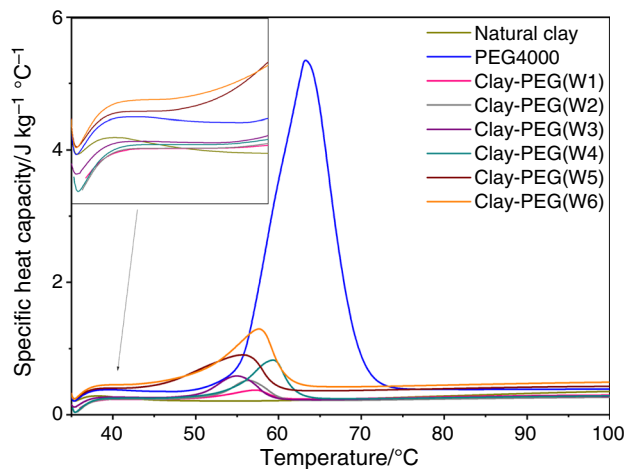
Fig. 8 Specific heat capacity associated with the raw clay, pure PEG and hybrids, at temperature ranging from 35 to 100℃

$$V_S = V_C - \frac{V_E}{\frac{P_1}{P_2} - 1}. \tag{10}$$

Then,

$$\rho_A = \frac{m_S}{V_S}. \tag{10a}$$

where, V_S, V_C, V_E, P_1 and P_2 are the sample volume, the volume of sample cell, the volume of expansion cell, the initial and the final pycnometer pressures, respectively.

Figure 9 shows the variation of the absolute density, and associated uncertainties, of the seven studied composite materials based on natural clay with different percentages of polymer (0%, 0.6%, 1.2%, 1.8 %, 2.5%, 2.8% and 3.1%). It can be noted that the incorporation of PEG chains in the clay matrix leads to a remarkable reduction in the absolute density of the hybrid from 2739.5 to 2618.6 kg m^{-3}, which allows again in the lightness of about 4.4% for the sample containing 2.8% of polymer. This reduction is mainly due to
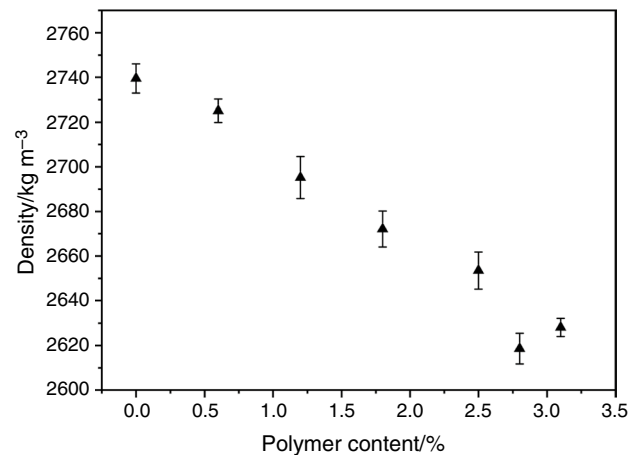
Fig. 9 The absolute density of raw clay and hybrids

the addition of PEG chains. The obtained result proves that those hybrid materials have to be considered as a promising materials for the thermal insulation sector.

Thermal conductivity measurements

The thermal conductivity, denoted as λ, is one of the main parameters which expresses the thermal performance of an insulation material. It is a function of the mineralogical compositions, or more specifically, the thermal conductivities of the individual components, and several textural features, such as the porosity degree, grain shape and grain size.

In Fig. 10, we report the experimental values of the thermal conductivity, and corresponding uncertainties, for several polymer contents. As illustration, we give, in Table 3, this thermal conductivity, for several values of the polymer content. We remark, from Fig. 10, the existence of *three* concentration regimes of the evolution of the thermal conductivity, when the polymer content varies from 0 to 3.1 %. Before discussing these phases, we note that the thermal conductivity of hybrids, λ, remains naturally below that of the raw clay, λ_c.

Table 2 Values of the thermal characteristics of raw clay, pure PEG and hybrids, from DSC analysis

Samples	Heating from 20 to 120/℃				Cooling from 120 to 20/℃			
	T_{start}	T_{onset}-T_{end}	T_{peak}	ΔH	T_{start}	T_{onset}-T_{end}	TT_{peak}	ΔH
	/℃	/℃	/℃	/Jg^{-1}	/℃	/℃	/℃	/Jg^{-1}
PEG4000	43.2	55.3-83.8	63.2	181.3	49.9	34.5-22.1	33.2	− 159.7
Clay-PEG$_{(w_1)}$	40.0	50.8-64.9	57.1	3.3	37.6	34.6-22.3	29.9	− 0.9
Clay-PEG$_{(w_2)}$	40.0	52.1-66.8	56.4	7.1	41.0	35.3-21.6	31.4	− 4.7
Clay-PEG$_{(w_3)}$	43.5	50.3-62.5	55.0	7.5	43.3	36.8-22.0	34.6	− 6.4
Clay-PEG$_{(w_4)}$	44.3	54.0-67.0	59.3	12.2	44.4	36.0-24.5	32.9	− 11.1
Clay-PEG$_{(w_5)}$	41.3	45.5-64.4	55.7	13.3	45.0	35.3-22.4	30.2	− 12.4
Clay-PEG$_{(w_6)}$	39.0	49.9-66.6	57.6	15.8	55.0	36.5-23.0	33.2	− 14.6
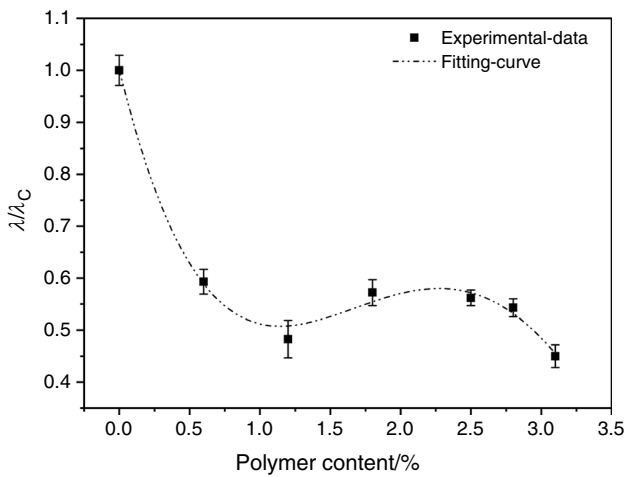
Fig. 10 Thermal conductivity of raw clay and hybrids

For polymer percentage below 1.2 % (very small fractions), that is for $w_i \leq 1.2$ %, λ naturally decreases, due to the fact that the presence of polymer reduces the thermal conductivity.

For polymer percentage between 1.2 % and 2.5 % (relatively small fractions), that is for $1.2 < w_i \leq 2.5$ %, λ increases. In this regime, we expect that there is no free polymer chains in samples, that is to say, initially, all of the polymer chains are either intercalated between clay layers or adsorbed on the clay grains surfaces.

For intermediate polymer contents, that is for $2.5 < w_i < w_i^* = 2.9$ % (w_i^* denotes the overlap polymer mass fraction, above which the initial polymer solution is semi-dilute), one assists to a decreasing of λ, due to an excess of free polymer chains.

In order to model the above behaviors of the thermal conductivity, λ, upon the polymer mass fraction $\left(w_i < w_i^*\right)$, the first step consists to write it as

$$\lambda = \lambda_c f\left(\frac{w_i}{w_i^*}\right), \tag{11}$$

The appearance of variable w_i/w_i^* in equality above is normal, since the ratio λ/λ_c is a dimensionless quantity. As second step, we assume that the function $f(x)$ is analytic of its argument, x. Then, to *third-order* in the polymer mass fraction, $w_i < w_i^*$, the thermal conductivity reads

$$\lambda = \lambda_c\left(1 - \alpha w_i + \beta w_i^2 - \delta w_i^3\right), \qquad w_i < w_i^*, \tag{12}$$

with the positive constants α, β and δ. We note that the above relation resembles the traditional virial expansion, usually encountered in fluid thermodynamics. Notice that these parameters increase with the polymerization degree of PEG, N, and scale as

$$\alpha \sim \left(w_i^*\right)^{-1} \sim N^{4/5}, \quad \beta \sim \left(w_i^*\right)^{-2} \sim N^{8/5}, \quad \delta \sim \left(w_i^*\right)^{-3} \sim N^{12/5}. \tag{12a}$$

A good fit with experimental data yields the following values of the above parameters,

$$\alpha = 0.9930 \pm 0.1369, \quad \beta = 0.5815 \pm 0.1930, \quad \delta = 0.1025 \pm 0.0933. \tag{12b}$$

For high polymer contents, that is for $w_i > w_i^*$ (the initial polymer solution was semi-dilute), the thermal conductivity also decreases, but the above virial expansion is no longer valid. In this fraction regime, due to an abundance of free PEG chains, we expect that the thermal conductivity decreases rapidly with the polymer-mass-fraction, according to a law of *parallel-model* type, that is

$$\lambda = \lambda_p v_p + \lambda_c v_c. \tag{13}$$

Here, v_p and $v_c = 1 - v_p$ are the volume-fractions of the two phases (pure polymer and natural clay). Since the volume-fraction, v_p, is directly proportional to the polymer-mass-fraction, the above expression may be rewritten as

$$\lambda = A_0 + B_0 w_i, \tag{13a}$$

with the known constants $A_0 > 0$ and $B_0 < 0$.

Finally, it is found that the experimental curve of the thermal conductivity (Fig. 10) agrees well with its proposed expressions (12) and (13a).

Table 3 Values of the absolute density, thermal conductivity, specific heat capacity and thermal diffusivity of raw clay, pure PEG and their hybrids

Samples	density /kg m^{-3}	Thermal conductivity /W $m^{-1}K^{-1}$	Specific heat capacity /J kg^{-1} K^{-1}	Thermal diffusivity /m^2 s^{-1} ($\times 10^{-7}$)
Raw clay	2739.5±6.5	0.631±0.029	283.96±0.03	8.099±0.069
PEG4000	1150.5±2.7	0.273±0.013	358.04±0.02	6.627±0.057
clay-PEG$_{(w_1)}$	2725.1±5.2	0.374±0.024	237.01±0.05	5.729±0.088
clay-PEG$_{(w_2)}$	2695.2±9.4	0.301±0.036	238.61±0.03	4.665±0.044
clay-PEG$_{(w_3)}$	2672.1±8.1	0.367±0.025	259.85±0.04	5.185±0.054
clay-PEG$_{(w_4)}$	2653.5±8.3	0.351±0.015	262.19±0.04	5.031±0.054
clay-PEG$_{(w_5)}$	2618.6±6.9	0.347±0.017	409.89±0.04	3.168±0.022
clay-PEG$_{(w_6)}$	2628.1±4.1	0.282±0.022	456.92±0.03	2.332±0.012

Specific heat capacity measurements

Figure 11 shows the variation of the ratio of the heat capacity of the composite, C_P, to that of the raw clay, C_{Pa}, versus the polymer content and the associated uncertainties. Table 4 lists the specific heat capacity values in the temperature range $0 - 45°C$. From these experimental data, one can see that the heat capacities of the fabricated hybrids increase with increasing polymer concentration. It is observed that, at temperatures below 45°C, the heat capacities of hybrids 1 to 4 become less pronounced in comparison with the raw clay; however, they exhibit a stable profile. This happened due to the effect of the polymer adsorption onto the clay layers.

In fact, at low polymer concentration, the polymer chains tend to form bridges between two closed clay surfaces. By raising the temperature, higher molecular vibration is provided, and then, the specific heat capacity of sample becomes less significant. In the case of higher polymer contents (hybrid 5 and hybrid 6), a new encapsulated sandwich structure confining polymer bilayers, is constructed. As a result, the system is trapped in a network and the thermal agitation decrease, leading to an increase of the heat capacity, compared with the pure PEG.

As for the thermal conductivity, we show that the heat capacity, C_P, can be given by the following virial expansion

$$C_P = C_{Pa}\left(1 - \alpha' w_i + \beta' w_i^2 + \delta' w_i^3\right), \tag{14}$$

with the heat-capacity of the pure clay, C_{Pa}, and the positive constants α', β' and δ'. As before, notice that these parameters increase with the polymerization-degree of PEG, N, and scale as

$$\alpha' \sim \left(w_i^*\right)^{-1} \sim N^{4/5}, \ \beta' \sim \left(w_i^*\right)^{-2} \sim N^{8/5}, \ \delta' \sim \left(w_i^*\right)^{-3} \sim N^{12/5}. \tag{14a}$$

1.7
1.6 ● Experimental-data
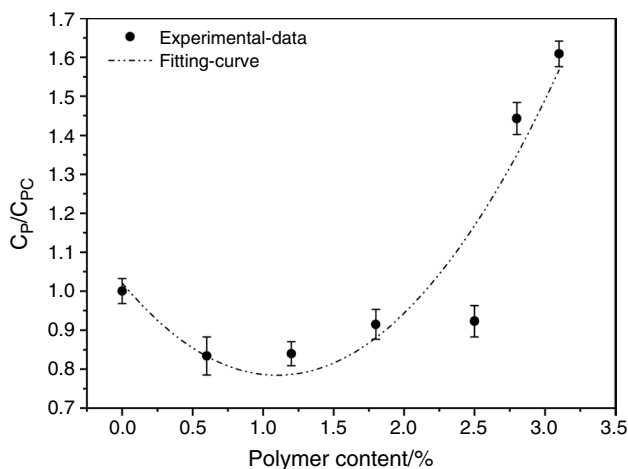   ---- Fitting-curve
1.5
1.4
1.3
1.2
1.1
1.0
0.9
0.8
0.7

Fig. 11 Heat capacity of raw clay and hybrids

A good fit with experimental data yields the following values of the above parameters,

$$\alpha' = 0.0974 \pm 0.1055, \ \beta' = 0.1285 \pm 0.1607, \ \delta' = 0.0732 \pm 0.0493. \tag{14b}$$

Finally, the experimental curve (Fig. 11) of the heat capacity is conform to that from modeling, relation (14).

Thermal diffusivity determination

The thermal diffusivity, D, is a physical quantity, characterizing the ability of a continuous material to transmit a temperature signal from one point to another inside it. In Table 3, we give the values of the thermal diffusivity of pure PEG, raw clay and hybrids, using formula (2). As indicated in this table, the thermal diffusivities of all of hybrids are below the thermal conductivity of the raw clay; this means that the polymer insertion in the clayey matrix enhances the thermal insulation properties of the raw clay. Also, this table stipules that the thermal diffusivity first decreases, with the polymer mass fraction, remain practically constant, for hybrids 2, 3 and 4, and falls, for higher polymer mass fractions.

In Fig. 12, we draw the thermal diffusivity, upon the polymer content. Such a curve reflects the discussion made above. As before, we state that this physical quantity can be modeled by the following virial expansion

$$D = D_c\left(1 - \alpha'' w_i + \beta'' w_i^2 - \delta'' w_i^3\right), \tag{15}$$

with the thermal diffusivity of raw clay, α_c, and the positive constants α'', β'' and δ''. These parameters increase with the polymerization-degree of PEG, N, according to

$$\alpha'' \sim \left(w_i^*\right)^{-1} \sim N^{4/5}, \beta'' \sim \left(w_i^*\right)^{-2} \sim N^{8/5}, \delta'' \sim \left(w_i^*\right)^{-3} \sim N^{12/5}. \tag{15a}$$

A best fit with experimental data gives the following values of the above parameters,

$$\alpha'' = 0.7883 \pm 0.6316, \ \beta'' = 0.4386 \pm 0.8585,$$
$$\delta'' = 0.0849 \pm 0.3848. \tag{15b}$$

Finally, the experimental curve (Fig. 12) of the thermal diffusivity is in agreement with that from modeling, relation (15).

Thermal insulation performance study

In order to examine the future challenges of the new elaborated composite for thermal comfort in building, a comparison between the thermal conductivity and the heat capacity of samples have been performed. The evaluation of the thermal performance of the composite can also be done by reasoning on the thermal diffusivity.
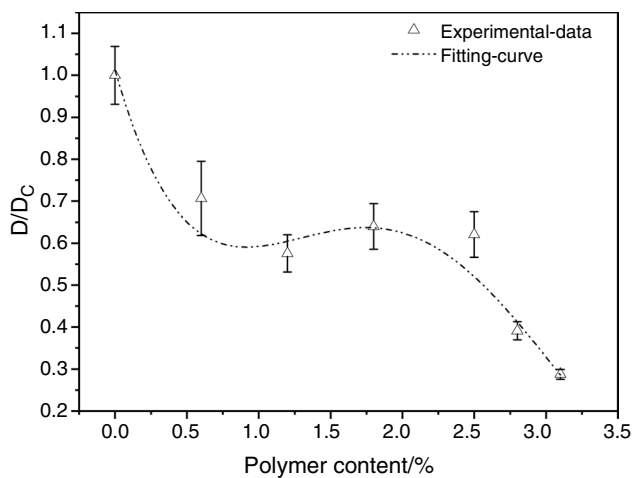
Fig. 12 Thermal diffusivity of raw clay and hybrids

Formula (2) then reveals that the magnitude of the thermal diffusivity, D, results from a competition between the thermal conductivity, λ, and the heat capacity, C_P, which mainly depend, for example, on the polymer content, the amount and the pores size present in the elaborated material. From a practical point of view, for thermal insulation purposes, it is interesting to choose materials with low thermal diffusivity.

According to Table 3, the thermal diffusivity as well as the thermal conductivity of the hybrids decrease from 8.099×10^{-7} m^{2}s^{-1} (raw clay) to 2.332×10^{-7} m^{2}s^{-1} (the clay-based composite), with 3.1 % of polymer and from 0.63 Wm^{-1}K^{-1} up to 0.28 Wm^{-1}K^{-1}, respectively. In general, the low value of thermal conductivity is associated with the appearance of additional pores or voids in the clay matrix which, contribute to improves the discontinuity of the thermal transport pathways due to the low conductivity of the air (0.0262 Wm^{-1}K^{-1}). This result is previously confirmed by SEM observation. In addition, this drop in thermal conductivity can be due to the insertion of the

polymeric reinforcement characterized by its low thermal conductivity 0.27 Wm^{-1}K^{-1}.

In Fig. 13, we superimpose the experimental variations of thermal conductivity and heat capacity, as a function of the amount of polymeric reinforcement, to determine the threshold value for the polymer content that gives improved thermal insulation performance.

From these curves, the two thermophysical quantities studied are practically constant (plateau regime), for a moderate range of polymer content starting from 1.2 to 2.5 %. Within this range, the corresponding thermal diffusivity is almost constant, while thermal conductivity and heat capacity vary from 0.30 to 0.35 Wm^{-1}K^{-1} and from 238.6 to 262.2 Jkg^{-1}K^{-1}, respectively.

For polymer content greater than 2.5 %, the thermal conductivity and thermal capacity of the composite reach their minimum and maximum values, respectively. Therefore, it can be concluded that the thermal performance of the composite is assured only for polymer contents above a threshold value $w^< = 2.5$ %. The present study suggests, then, that the best thermophysical values of the composite produced should be $\lambda^{op} = 0.28$ Wm^{-1}K^{-1} and $C_p^{op} = 456.92$ Jkg^{-1} K^{-1}, corresponding to hybrid 6.

The production cost was reduced by using less chemical components and more clay as an indigenous and economical resource and also by using a simple and non-toxic process with relatively low temperature conditions. Being non-toxic in nature, economical, high insulation potential and high thermal stability, the composites developed in this work are suitable to be encapsulated in the building envelope, as ecological insulator with good thermophysical properties.

Finally, Table 4 lists the comparison of the thermophysical properties of the fabricated clay-PEG-hybrids with those of common building materials and composites insulators in literature [40–44]. Based on the data in this table, it is interesting to note that the new fabricated composite has an important potential for thermal insulation application in building envelope.

Table 4 Thermal diffusivity of raw clay and hybrids

Materials	Thermal conductivity /W m^{-1}K^{-1}	Specific heat capacity /J kg^{-1}K^{-1}	References
Brick	0.69	835.23	[40]
Cement plaster	0.72	840.00	[41]
Clay mixture brick	0.35	821.60	[42]
Clay-wool (5%)	0.51	499.42	[43]
Clay-PEG4000 (3.1%)	0.28	456.92	This work

Fig. 13 Superposition of the thermal conductivity and heat capacity relatively to raw clay and hybrids
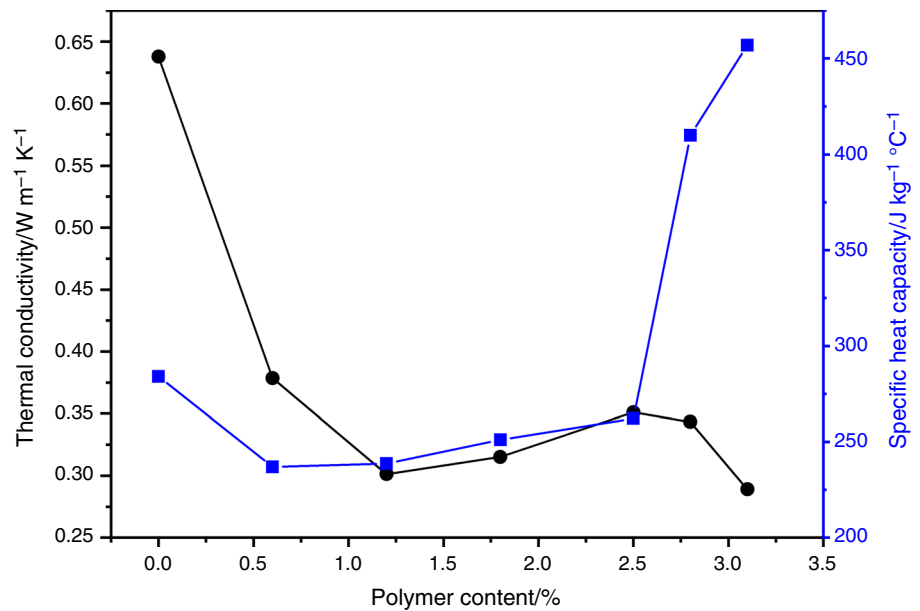
Conclusions

Recently, Morocco has been engaged in an extensive sustainable development, especially in the field of energy efficiency. Within this context, clay-based insulators, with low environmental impact, contribute to a reduction of energy demand for heating and cooling, because of their remarkable thermophysical characteristics.

We recall that, this paper has given an account of new thermal insulation material based on raw clay, which have been developed by incorporating PEG chains into the clay layers using the intercalation from solution method. These new elaborated hybrids, made of natural clay and PEG, are thermophysically characterized in an attempt to analyze their thermal behavior, by adding different amount of the polymer chains. To this end, the characterization of different samples was provided using many experimental techniques, as SEM, DTA, TGA and DSC analyses. Furthermore, theoretical modeling and mathematical treatment of thermal degradation versus temperature and time were implemented and compared with TGA measurements. On the other hand, experimental procedures consist of different apparatus (helium pycnometer, guarded heat flow meter, DSC instrument) were used in an attempt to determine the material properties such as $\left(\rho_A, \lambda, C_p\right)$. These measurements were modeled based on the traditional virial law and analyzed in order to evaluate the challenge of the new hybrid to be applied as thermal insulator for building. This work leads to the following outcomes:

– The incorporation of PEG chains into the clay matrix alters the surface morphology of the raw clay from a hazardous dispersion of phases to well-defined structures.

Also, the SEM analysis shows connections between clay particles for a polymer content of 2.5% due to the great adhesion between the PEG chains and the clay platelets.
– For temperatures below 50°C, the TGA measurements and DSC analysis show improved thermal stability and good thermal characteristics of the PEG-intercalated clay hybrids, respectively.
– The absolute densities of the new hybrid models decrease from 2739.5 to 2618.6 kgm^{-3}, which contribute in the lightness of about 4.4% for the hybrid sample containing 2.8% of polymer.
– The thermal conductivity of the hybrids is affected by the progressive addition of PEG chains and decreases from 0.631 to 0.282 Wm^{-1}K^{-1}. Moreover, its variation can be modeled by virial expansions and we find that the theoretical modeling agrees with the experiment.
– The specific heat capacity for the hybrids increases by increasing the polymeric reinforcement in the cay matrix, it shows a maximum value of 456.92 Jkg^{-1}K^{-1} for the hybrid with 3.1% of polymer content.
– The thermal diffusivity of each hybrid sample is calculated from the thermophysical properties ρ_A, λ and C_p. The obtained result shows that the thermal diffusivity of the hybrids decreases in comparison with that of the raw clay and varies from 8.099×10^{-7} to 2.332×10^{-7} m^{2}s^{-1}.
– By comparing the thermal conductivity and specific heat capacity variations, one can see that there is a threshold value of 2.5%, above which the thermal insulation properties are enhanced.
– All these thermal characteristics make the elaborated composite a suitable material for the thermal insulation in building, in comparison with other reported insulation materials.

Finally, the association of this natural clay with an appropriate hydro-soluble polymer as PEG gives rise not only to much better thermal insulation performance, but also to new eco-friendly insulator for building and construction industry.

Declarations

Conflict of interest There are no conflicts to declare.

References

1. Chen GQ, Wu XD, Guo J, Meng J, Li C, Global overview for energy use of the world economy: Household-consumption-based accounting based on the world input-output database (WIOD). Energy Econ. 2019; 81: 835–47.
2. Pedroso M, Flores-Colen I, Silvestre JD, Gomes MG, Silva L, Sequeira P, De Brito J (2020) Characterisation of a multilayer external wall thermal insulation system. Application in a Mediterranean climate. J Build Eng. 30: 101265-301.
3. Leng G, Zhang X, Shi T, Chen G, Wu X, Liu Y, Fang M, Min X, Huang Z, Preparation and properties of polystyrene/silica fibres flexible thermal insulation materials by centrifugal spinning. Polymer 2019; 185; 121964–991.
4. Jia G, Li Z, Liu P, Jing Q, Preparation and characterization of aerogel/expanded perlite composite as building thermal insulation material. J. Non-Cryst. Solids 2018;482: 192–202.
5. Zeng Q, Mao T, Li H, Peng Y. Thermally insulating lightweight cement-based composites incorporating glass beads and nano-silica aerogels for sustainably energy-saving buildings. Energy Build. 2018; 174:97–110.
6. Govan FA, editor. Thermal Insulation, Materials, and Systems for Energy Conservation in the'80s. ASTM International; 1983.
7. Naldzhiev D, Mumovic D, Strlic M. Polyurethane insulation and household products-a systematic review of their impact on indoor environmental quality. Build Environ. 2020; 169: 106559.
8. Aditya L, Mahlia TM, Rismanchi B, Ng HM, Hasan MH, Metselaar HS, Muraza O, Aditya HB. A review on insulation materials for energy conservation in buildings. Renew. Sustain. Energy Rev. 2017; 73: 1352–65.
9. He YL, Xie T. Advances of thermal conductivity models of nanoscale silica aerogel insulation material. Appl. Therm. Eng. 2015; 81: 28–50.
10. Torres-Rivas A, Palumbo M, Haddad A, Cabeza LF, Jiménez L, Boer D. Multi-objective optimisation of bio-based thermal insulation materials in building envelopes considering condensation risk. Appl. Energy. 2018; 224: 602–14.
11. An W, Wang Z, Xiao H, Sun J, Liew KM. Thermal and fire risk analysis of typical insulation material in a high elevation area: Influence of sidewalls, dimension and pressure. Energy Convers. Manag. 2014; 88: 516–24.
12. Stec AA, Hull TR. Assessment of the fire toxicity of building insulation materials. Energy Build. 2011; 43: 498–06.
13. Lachheb A, Allouhi A, El Marhoune M, Saadani R, Kousksou T, Jamil A, Rahmoune M, Oussouaddi O. Thermal insulation improvement in construction materials by adding spent coffee grounds: An experimental and simulation study. J. Clean. Prod. 2019; 209: 1411–9.
14. Kairytė A, Kremensas A, Balčiūnas G, Matulaitienė I, Członka S, Sienkiewicz N. Evaluation of self-thermally treated wood plastic composites from wood bark and rapeseed oil-based binder. Constr. Build. Mater. 2020; 250: 118842.
15. Boukhattem L, Boumhaout M, Hamdi H, Benhamou B, Nouh FA. Moisture content influence on the thermal conductivity of insulating building materials made from date palm fibers mesh. Constr. Build. Mater. 2017; 148: 811–23.
16. Shabtai IA, Mishael YG. Catalytic polymer-clay composite for enhanced removal and degradation of diazinon. J. Hazard. Mater. 2017; 335: 135–42.
17. Da Cunha SR, De Aguiar JL. Phase change materials and energy efficiency of buildings: A review of knowledge. J. Energy Storage. 2020; 27: 101083.
18. Pisello AL. Thermal-energy analysis of roof cool clay tiles for application in historic buildings and cities. Sustain. Cities Soc. 2015; 19: 271–80.
19. Rathore PK, Shukla SK, Gupta NK. Potential of microencapsulated PCM for energy savings in buildings: A critical review. Sustain. Cities Soc. 2020; 53: 101884.
20. Sutcu M, Del Coz Díaz JJ, Rabanal FP, Gencel O, Akkurt S. Thermal performance optimization of hollow clay bricks made up of paper waste. Energy Build. 2014; 75: 96–108.
21. Hu F, Wu S, Sun Y. Hollow- structured materials for thermal insulation. J. Adv. Mater. 2019; 31: 1801001.
22. Gupta P, Verma C, Maji PK. Flame retardant and thermally insulating clay based aerogel facilitated by cellulose nanofibers. J. Supercrit. Fluids. 2019; 152: 104537.
23. Estravís S, Tirado-Mediavilla J, Santiago-Calvo M, Ruiz-Herrero JL, Villafañe F, Rodríguez-Pérez MÁ. Rigid polyurethane foams with infused nanoclays: relationship between cellular structure and thermal conductivity. Eur. Polym. J. 2016; 80: 1–5.
24. Xu JZ, Gao BZ, Kang FY. A reconstruction of Maxwell model for effective thermal conductivity of composite materials. Appl. Therm. Eng. 2016; 102: 972–9.
25. Sundstrom DW, Lee YD. Thermal conductivity of polymers filled with particulate solids. J. Appl. Polym. Sci. 1972; 16: 3159–67.
26. Agari Y, Tanaka M, Nagai S, Uno T. Thermal conductivity of a polymer composite filled with mixtures of particles. J. Appl. Polym. Sci. 1987; 34: 1429–37.
27. Kucukdogan N, Aydin L, Sutcu M. Theoretical and empirical thermal conductivity models of red mud filled polymer composites. Thermochim. Acta. 2018; 665: 76–84.
28. Reeves GM, Sims I, Cripps JC, editors. Clay materials used in construction. Geological Society of London; 2006.
29. Ghyati S, Kassou S, El Jai M, Benhamou M. Investigation of PEG4000/Natural clay-based hybrids: Elaboration, characterization and theory. Mater. Chem. Phys. 2020; 239: 121993.
30. Suresh K, Pugazhenthi G, Uppaluri R. Properties of polystyrene (PS)/Co-Al LDH nanocomposites prepared by melt intercalation. Mater. Today-Proc. 2019; 9: 333–50.
31. Zhang G, Wu T, Lin W, Tan Y, Chen R, Huang Z, Yin X, Qu J. Preparation of polymer/clay nanocomposites via melt intercalation under continuous elongation flow. Compos. Sci. Technol. 2017; 145: 157–64.
32. Puffr R, Špátová JL, Brožek J. Clay mineral/polyamide nanocomposites obtained by in-situ polymerization or melt intercalation. Appl. Clay. Sci. 2013; 83: 294–9.
33. Ramakumar K, Saxena M, Deb S. Experimental evaluation of procedures for heat capacity measurement by differential scanning calorimetry. J. Therm. Anal. Calorim. 2001; 66:387–97.
34. Nguyen HG, Horn JC, Bleakney M, Siderius DW, Espinal L. Understanding material characteristics through signature traits from helium pycnometry. Langmuir. 2019; 35: 2115–22.

35. Standard AS. Standard Test Method for Evaluating the Resistance to Thermal Transmission of Materials by the Guarded Heat Flow Meter Technique. Designation: E1530–11. 2011.

36. Verhulst PF, *Deuxième mémoire sur la loi d'accroissement de la population*, Mémoire de l'Academie Royale des Sciences et des Lettres et des Beaux-Arts de Belgique. 1847; 20:1-32.

37. Bohor BF, Hughes RE. Scanning electron microscopy of clays and clay minerals. Clay Miner. 1971; 19: 49–54.

38. Zampori L, Dotelli G, Stampino PG, Cristiani C, Zorzi F, Finocchio E. Thermal characterization of a montmorillonite, modified with polyethylene-glycols (PEG1500 and PEG4000), by in situ HT-XRD and FT IR: Formation of a high-temperature phase. Appl. Clay Sci. 2012; 59: 140–7.

39. Amziane S, Collet F, Lawrence M, Magniont C, Picandet V, Sonebi M. Recommendation of the RILEM TC 236-BBM: characterisation testing of hemp shiv to determine the initial water content, water absorption, dry density, particle size distribution and thermal conductivity. Mater. Struct. 2017; 50: 1–1.

40. Sutcu M, Akkurt S. The use of recycled paper processing residues in making porous brick with reduced thermal conductivity. Ceram. Int. 2009; 35: 2625–31.

41. Gounni A, Mabrouk MT, El Wazna M, Kheiri A, El Alami M, El Bouari A, Cherkaoui O. Thermal and economic evaluation of new insulation materials for building envelope based on textile waste. Appl. Therm. Eng. 2019; 149: 475–83.

42. Laaroussi N, Cherki A, Garoum M, Khabbazi A, Feiz A. Thermal properties of a sample prepared using mixtures of clay bricks. Energy Procedia. 2013; 42: 337–46.

43. Mounir S, Khabbazi A, Khaldoun A, Maaloufa Y, El Hamdouni Y. Thermal inertia and thermal properties of the composite material clay-wool. Sustain. Cities Soc. 2015; 19: 191–9.